THE JOURNAL OF PHYSICAL CHEMISTRY B

ARTICLE

pubs.acs.org/JPCB

A Local Entropic Signature of Specific Ion Hydration

Thomas L. Beck*

Department of Chemistry and Department of Physics, University of Cincinnati, Cincinnati, Ohio 45221-0172, United States

ABSTRACT: Monovalent ion hydration entropies are analyzed via energetic partitioning of the potential distribution theorem free energy. Extensive molecular dynamics simulations and free energy calculations are performed over a range of temperatures to determine the electrostatic and van der Waals components of the entropy. The far-field electrostatic contribution is negative and small in magnitude, and it does not vary significantly as a function of ion size, consistent with dielectric models. The local electrostatic contribution, however, varies widely as a function of ion size; the sign yields a direct indication of the kosmotropic (strongly hydrated) or chaotropic (weakly hydrated) nature of the ion hydration. The results provide a thermodynamic signature for specific ion effects in hydration and are consistent with experiments that suggest minimal perturbations of water structure outside the first hydration shell. The hydration entropies are also examined in relation to the corresponding entropies for the isoelectronic rare gas pairs; an inverse correlation is observed, as expected from thermodynamic hydration data.

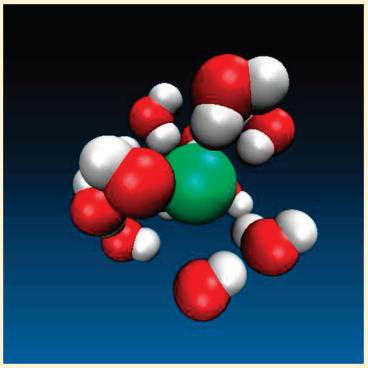

INTRODUCTION

Entropic contributions ($-Ts^{ex}$) to ion hydration free energies are typically small relative to the enthalpic components (h^{ex}).[1−8] This observation is often rationalized by invoking a competition between increased water order due to the strong ion−water interactions and decreased water order due to the disruption of the water−water hydrogen-bond network.[1,9,10] A further point of interest is that the hydration entropy of dilute KCl is close to that for two (isoelectronic) argon atoms.[1,2] While the hydration free energy exhibits ion-specific behavior, with larger ions typically displaying smaller magnitude free energies, the hydration entropy provides a more direct connection to ordering effects due to ion insertion into water. This paper addresses, through molecular dynamics simulations and entropy calculations, specific ion effects in ion hydration. By partitioning the entropy into van der Waals and local and far-field electrostatics contributions, a clear entropic signature for the kosmotropic/chaotropic distinction emerges from the sign of the local electrostatic contribution to the hydration entropy. For the present discussion, the terms kosmotrope (strongly hydrated) and chaotrope (weakly hydrated) are used solely to refer to the nature of the local hydration structure and thermodynamics, as discussed in ref 9; these terms are often more generally used to reflect a wider range of bulk solution behaviors.[8]

It is helpful to physically partition hydration problems into local and far-field components. Two such partitionings have appeared, the quasi-chemical[11−20] and local molecular field theories[21−25] (QCT and LMFT, respectively). In the QCT, the hydration free energy is spatially partitioned into inner-shell and outer-shell parts in the following three-step thermodynamic process: (1) cavity creation (outer-shell packing); (2) solute insertion into the cavity (outer-shell long-ranged contribution); and (3) relaxation of the cavity constraint (inner-shell chemical contribution). Subsequent judicious physical approximations can then be made; for example, the outer-shell long-ranged contribution might be modeled at a dielectric continuum or classical molecular dynamics level, while the inner-shell term requires a molecular-level, perhaps quantum treatment. The alternative LMFT has focused on partitioning the electrostatic interactions into local and far-field contributions similar to the Ewald method. That theory has mainly been applied to fluid and interface structure, with some work directed at computations of thermodynamic quantities, such as the internal energy and pressure.[24]

The QCT and LMFT approaches have been related by energetic partitioning of the potential distribution theorem (PDT)[26] free energy.[27] The resulting exact separation divides the hydration free energy into the following three parts: (1) a van der Waals contribution that is the free energy to insert an uncharged ion; (2) the local electrostatic contribution that corresponds to turning on the ion−water local electrostatic interactions; and (3) the far-field electrostatic contribution that results from turning on the remaining ion−water electrostatic interactions. By sampling in multiple states, accurate estimates for ion hydration free energies were obtained from the distributions of interaction energies. In addition, for electrostatic damping lengths on the order of 4 Å, the distribution of interaction energies for the far-field electrostatic contribution is accurately Gaussian. This finding is consistent with dielectric models for that far-field contribution. Gaussian models that include all the electrostatic interactions are not generally accurate,[27] however, so the local contributions to the free energy need to be computed directly.

The paper is organized as follows. The theory is first briefly summarized to set the stage for the entropy calculations. The computational methods employed in the simulations are then

Received: May 25, 2011
Revised: June 29, 2011
Published: July 05, 2011

discussed. The results of the entropy calculations are presented, and the results are discussed in the context of previous work on ion hydration entropies. Finally, the conclusions are summarized.

THEORY

The local contribution to the electrostatic interaction energy is taken as the following:[23]

$$u_{es,loc}(r_{ij}) = \frac{q_i q_j \ \mathrm{erfc}(\eta r_{ij})}{r_{ij}} \quad (1)$$

where $1/\eta$ is the damping length. In the present work, that length is taken just outside the first minimum of the X−O radial distribution function, where X is an anion and O is the water oxygen, or just outside the first minimum of the X−H radial distribution function, where X is a cation and H is the water hydrogen. The complementary error function damps the electrostatic interactions to 16% of the undamped value at the distance $1/\eta$, so the chosen damping lengths lead to the inclusion of the interactions mainly from the first hydration shell around the ions. With these $1/\eta$ values, the local and far-field electrostatic contributions to the free energy are of comparable magnitude.

We start from the inverse form of the PDT as follows:[26]

$$e^{\beta\mu^{ex}} = \langle e^{\beta\Delta U}\rangle \quad (2)$$

where $\beta = 1/kT$, μ^{ex} is the ion excess chemical potential, ΔU is the full interaction energy of the ion with the surrounding waters, and the sampling is conducted with the ion present. The hydration free energy can then be partitioned[27] as follows:

$$\beta\mu^{ex} = \beta\mu^{ex}_{LJ} + \ln\langle e^{\beta[\Delta U_{loc} - \Delta U_{LJ}]}\rangle_{\Delta U_{loc}} + \ln\langle e^{\beta[\Delta U - \Delta U_{loc}]}\rangle \quad (3)$$

The first term is the free energy to insert the uncharged ion into water. The interaction energy ΔU_{loc} includes the local electrostatic and van der Waals (vdW, here Lennard-Jones) interaction energies, so the second term yields the local electrostatic contribution to the free energy. The third term is the far-field electrostatic contribution to the free energy. The full electrostatic interactions are computed with the Ewald method.[20] The sampling in the second term is conducted on a Hamiltonian that includes the ΔU_{loc} interactions and all water−water interactions, while the sampling in the last term is performed with all interactions included. The water−water interactions are treated at the full Ewald level for all sampling states.

Perturbation theory[28] then suggests that the above equation can be rewritten as follows:

$$\beta\mu^{ex} = \beta\mu^{ex}_{LJ} - \ln\langle e^{-\beta[\Delta U_{loc} - \Delta U_{LJ}]}\rangle_{\Delta U_{LJ}} - \ln\langle e^{-\beta[\Delta U - \Delta U_{loc}]}\rangle_{\Delta U_{loc}} \quad (4)$$

Reference 27 uses the basic relation between the interaction energy distributions derived by Bennett,[20,29,30]

$$P_A(\varepsilon) = e^{-\beta[\varepsilon - \mu^{ex}_{AB}]} P_B(\varepsilon) \quad (5)$$

to construct the $P_A(\varepsilon)$ distribution over a wide energy range so that the inverse PDT expression can be directly integrated to yield the free energy for the B → A transition. A and B are the two different sampling states for the respective terms indicated in eqs 3 and 4, and ε is the energy difference $\Delta U_A - \Delta U_B$. In practice, an intermediate state for the local electrostatic component is required because of the strength of those local interactions; in total, four simulations are required to obtain the free energy (except the packing contribution, see below). It can also be noted that the crossing point of the two distributions already produces an estimate of the sought free energy change, and computational studies[27] have shown this estimate to be remarkably accurate.

Table 1. vdW Parameters and Chosen Damping Lengths[a]

ion	σ_{XW}	ε_{XW}	η^{-1}
F^-	3.05	0.1324	3.9
Cl^-	3.75	0.1286	4.5
Br^-	3.83	0.1182	4.8
I^-	4.20	0.1182	5.1
I^-_{lg}	4.50	0.1182	5.4
Na^+	2.85	0.0479	4.5
K^+	3.30	0.0591	4.8

[a] The σ_{XW} and η^{-1} values are in Å, and the ε_{XW} values are in kcal/mol.

COMPUTATIONAL METHODS

In the present study, the hydration free energies for seven ions are computed over a range of temperatures from 278 to 348 K in 10 K increments, following the above strategy. van′t Hoff analysis is performed to obtain the hydration entropies. The SPC model is employed for the water interactions, and for the most part, the ion−water vdW interactions were taken from ref 31. (The potential for the K^+ ion was modified by incorporating a more reasonable well depth, and the σ parameter was adjusted to yield a first maximum in the radial distribution function, rdf, that agrees with previous simulations.[32] The parameters for the I^- ion were adjusted to produce a first rdf maximum near that obtained in DFT simulations.[33] In addition, a slightly larger I^--like anion, labeled I^-_{lg}, was modeled.) The vdW parameters and damping lengths are listed in Table 1. The simulated systems included 214 water molecules and one ion located in a periodic box of size L = 18.643 Å. Constant temperature and volume conditions were employed. (The ensemble dependence of the computed entropies is expected to be weak for the problems examined here.) The systems were equilibrated for at least 500 ps, and production runs of 5 ns were performed for each temperature to obtain well converged free energies for the subsequent van′t Hoff analysis. All simulations were performed with the Tinker molecular dynamics package.[34,35]

The aim of the present work is to gain a first glimpse of local and far-field contributions to hydration entropies. The simple models employed here incorporate electrostatic effects in an average way. More subtle ordering effects due to ion polarization are not included and should be the subject of future work. For example, it is known that the degree of anion polarization influences the extent of local hydration asymmetry,[36] and those effects can be expected to alter the contributions to the entropy in nontrivial ways. In addition, charge transfer occurs in halide hydration.[37,38] The present study leads to insights into a dominant aspect of ion hydration, namely the electrostatic contribution. While no effort was made in this study to alter the model parameters to fit experimental hydration entropies, the results are in reasonably good agreement with experiment (with the exceptions of the F^- and I^- ions; see below). Other work has shown that nonpolarizable ion models can reproduce a wide range of ion hydration properties.[39−41] The main focus here is on the influence of ion size on the local and far-field electrostatic contributions to the entropy.

dx.doi.org/10.1021/jp204883h |J. Phys. Chem. B 2011, 115, 9776–9781

For the vdW component, the free energies are computed directly from QCT calculations.[20,36,42] The QCT form of the free energy is as follows:

$$\beta\mu_{LJ}^{ex} = \ln x_0(\lambda) - \ln p_0(\lambda) + \ln\langle e^{\beta\Delta U_{LJ}} | r > \lambda\rangle_{\Delta U_{LJ}} \qquad (6)$$

where x_0 is the probability of no water occupancy in the inner shell with the solute present and p_0 is the probability of no water occupancy in the inner shell with the solute absent. The three terms, in order, are (1) the inner-shell contribution (minus the free energy to move the inner-shell water molecules out to a distance λ), (2) the hard-sphere packing contribution (free energy to grow a cavity of size λ in bulk water), and (3) the long-ranged contribution (free energy to insert the solute into an existing cavity of size λ). The averaging in the long-ranged term is conditional on no water present in the inner shell. The first and third terms were calculated directly from simulation data for the vdW particles. The first term involves occupancy statistics for the inner-shell region; the spatial cutoff was taken at the value of the ion−water σ parameter. In refs 27 and 43, it was found that the third term can be computed accurately with a Gaussian model, and that approach is followed here. The entropy for the second (packing) term above was obtained from Figure 15 of ref 44.

RESULTS AND DISCUSSION

Figure 1 displays the temperature dependent (total) electrostatic free energy data for the six ions examined here: Na^+, K^+, F^-, Cl^-, Br^-, and I^- (the I_{lg}^- ion is omitted in this figure). It can be seen from the data and confirmed by linear regression that linear behavior is observed over the whole temperature range. The local and far-field components of the electrostatic part of the free energy display similarly linear behavior over the examined temperature range. The ordering of the electrostatic free energies in Figure 1 is the same as that for the experimental total free energy data from ref 6, except the Na^+ and Cl^- results are reversed; note, however, that Figure 1 does not include the vdW portion of the free energy.

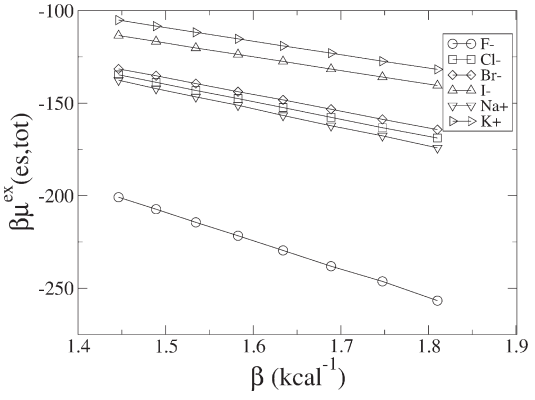

Figure 1. Temperature dependence of the total electrostatic contribution to hydration free energies.

The long-ranged vdW component computed with a Gaussian model also displays linear temperature dependent behavior. The inner-shell component, however, exhibits some nonlinearity, which is not surprising for this hydrophobic hydration problem. The data were thus fit to the functional form $\mu_{IS}^{ex} = c_0 + c_1 T + c_2(T \ln T)$, consistent with a constant heat capacity contribution.[44] The fit accurately reproduces the data, and the slope was used to estimate the corresponding entropy at 298 K. The data for the seven ions are presented in Table 2.

We start by discussing the entropy results for the uncharged ions, namely the LJ particles. It is well-known that the entropy of hydration of hard-sphere solutes (s_{HS}^{ex}) is negative, with the magnitude increasing with increasing particle size.[44] It is apparent from Table 2 that s_{HS}^{ex} is the largest contribution to the vdW particle entropy. The inner-shell contribution is positive, and the magnitude increases with increasing size, leading to a partial compensation for the packing term. The long-ranged component of the entropy is negative and small in magnitude, leading to little ion specificity. The total vdW entropy exhibits the expected general trend of larger magnitude negative values with increasing particle size (at room temperature—see ref 4, Table 2.22).[44]

We next focus on the far-field electrostatic contribution to the entropy. The data show that this component of the entropy is negative and exhibits relatively small variation with ion size. Reference 27 shows that the far-field term can be accurately modeled at the Gaussian level, and this is consistent with dielectric models. As discussed in ref 20 (Chapter 1), such a dielectric model predicts a small negative entropy mainly through the temperature dependence of the dielectric constant. Thus, the far-field term does not exhibit strong ion specificity. We note that there may be some system size dependence to the far-field term; in ref 27, a value for $s_{es,far}^{ex}$ for the Cl^- ion was estimated as -8.6 ± 4 cal/(mol K). That study involved 499 water molecules, but the entropy calculations were performed for shorter time scales and at fewer temperatures. Also, the damping length was taken as slightly smaller than that employed here; a shorter damping length emphasizes the far-field contribution. It is conceivable that the smaller system sizes examined here may

Table 2. Hydration Entropy Data[a]

ion	$s_{es,loc}^{ex}$	$s_{es,far}^{ex}$	$s_{es,tot}^{ex}$	s_{IS}^{ex}	s_{HS}^{ex}	s_{LR}^{ex}	s_{vdW}^{ex}	s_{tot}^{ex}	s^{ex}(expt)
F^-	−36.6(2.2)	−3.5(0.8)	−40.0(2.6)	5.4(0.1)	−14.2	−0.44(0.04)	−9.2	−49.2	−30.4
Cl^-	0.5(0.8)	−3.1(0.5)	−2.7(1.1)	10.8(0.3)	−22.0	−0.72(0.04)	−11.9	−14.6	−15.4
Br^-	3.9(0.8)	−2.2(0.3)	1.7(0.9)	12.2(0.4)	−22.9	−0.60(0.08)	−11.3	−9.6	−11.6
I^-	15.0(0.6)	−2.7(0.2)	12.4(0.7)	15.1(0.5)	−27.0	−0.76(0.17)	−12.7	−0.3	−7.3
I_{lg}^-	19.3(0.7)	−2.3(0.3)	17.0(0.8)	18.0(0.9)	−30.1	−0.86(0.16)	−13.0	4.0	
Na^+	−9.5(1.8)	−4.4(0.3)	−13.9(1.8)	6.6(0.1)	−12.2	−0.08(0.02)	−5.7	−19.6	−16.3
K^+	1.5(0.9)	−2.7(0.3)	−1.2(0.9)	9.1(0.2)	−16.9	−0.22(0.03)	−8.0	−9.1	−7.7

[a] In order, the listed entropies are the following: the local electrostatic contribution, the far-field electrostatic contribution, the total electrostatic contribution, the inner-shell vdW contribution, the hard-sphere packing vdW contribution, the long-ranged vdW contribution, the total vdW contribution, the computed total entropy of hydration, and the experimental data obtained from ref 6. The inner-shell, hard-sphere packing, total vdW, computed total, and experimental data are at room temperature. Error estimates are listed in parentheses. All values are in cal/(mol K).

lead to a slight underestimation of the far-field entropy as a result of limitations on the (small) induced water orientations further from the ion. Thus, the far-field (and resulting total) estimated entropies may be uniformly shifted to more negative values by a few cal/(mol K) in the large size limit. (The local electrostatic contribution to the entropy is very close to that estimated in ref 27.)

The local electrostatic contribution to the entropy, on the other hand, displays wide variation with ion size. Small ions exhibit negative values for this entropic contribution, while large ions display positive values. On the basis of this observation, it is apparent that ion specificity in the hydration entropy arises largely from $s^{ex}_{es,loc}$. A physical interpretation is that small ions with high charge densities lead to significant ordering of the nearby waters that can overcome any reduced order caused by disruption of the local water-water hydrogen-bonding network. The electrostatic field of larger ions with lower charge densities likely does orient nearby waters to some extent, but apparently, there exists a competition[45] (or "frustration"[46]) between hydrophilic and hydrophobic hydration effects that leads to increased disruption of the local water−water hydrogen-bonded network and the observed positive sign, in contrast with purely hydrophobic hydration. The results provide a thermodynamic connection to spectroscopic[47] and other[45,48] studies that have found minimal perturbations beyond the first hydration shell. There is some ordering of water dipoles in the far field that leads to the small magnitude negative entropy values, but those perturbations to the overall structure are likely minor.

These results help to explain the different trends apparent from experimental entropy data on ion vs rare gas hydration. For rare gases, the entropy becomes more negative with increasing atom size at room temperature,[4,49] indicating that water reorders in some way so as to maintain its hydrogen-bonding network around the hydrophobic particle. (This is not to suggest the formation of iceberglike structures[50] around the nonpolar solutes, however; computational studies have shown significantly anisotropic local hydration structures around nonpolar solutes that differ from clathrate structures.[42,51]) Ions display the opposite trend, with the hydration entropy becoming less negative with increasing ion size. The large (and somewhat counterintuitive) positive values for $s^{ex}_{es,loc}$ are the cause of the observed trend with increasing ion size. The observation that the *total* electrostatic contribution can be positive for the larger anions gives an indication of the strong influence of the local electrostatic part of the entropy.

In general, the agreement between the computed entropies and the experiment is quite good, considering the extreme simplicity of the models employed here. The two exceptions are the F^- and I^- ions at the extremes of the anion size range. It is tempting to speculate that the difficulties for these ions are due to different causes. The F^- ion exhibits several well-known anomalies in relation to the other halides.[9,52−54] The hydration free energy is of large magnitude, reflecting strong chemical interactions (involving charge rearrangements). The simple point charge models employed here cannot be expected to capture those chemical effects. In addition, because the ions and waters only include repulsive vdW interactions between the ions and oxygens in the models employed here, the protons can penetrate closer to the anion nucleus.[31] This effect can be expected to be more prominent for smaller anions. Finally, the current F^- model results in a computed hydration free energy of −139.3 kcal/mol at room temperature, compared with the experimental result[6] of −119.7 kcal/mol, which provides a further indication of overhydration in the model. On the other hand, the present fixed charge models do not incorporate any contribution from ion polarization. Because the I^- is the most polarizable of the examined halide series, it can be expected that inclusion of polarization may lead to a more negative result for the entropy due to ordering caused by the anion dipole/water interactions.

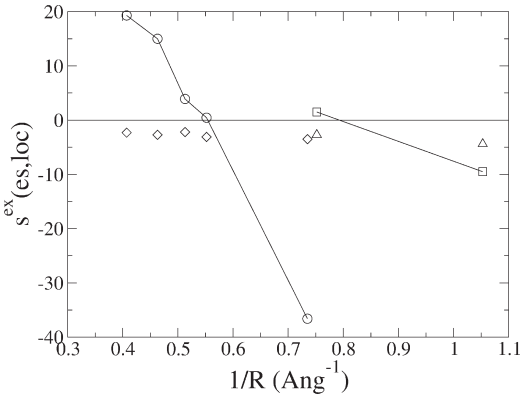

Figure 2. Size dependence of the local and far-field electrostatic contributions to hydration entropies. Ion size is taken as the Pauling crystal radius.[58] (Left) Anion series (circles for local contributions and diamonds for far-field contributions). (Right) Cation data (squares for local contributions and triangles for far-field contributions).

The extensive literature on ion solvation includes previous attempts to separate out local, structural aspects of hydration entropies.[1,3,5,8,48,50] One example is Marcus's definition[3] of a structural entropy as the measured hydration entropy minus the sum of an estimated Born energy and a nonelectrostatic and nonstructural contribution. He notes a sign change for this quantity along the halide series, with F^- exhibiting a large negative value and Cl^-, Br^-, and I^- displaying positive values increasing with ion size. Another example is ΔS_{II} defined by Krestov,[5] which is the difference between the partial molar entropy of the ion and that for water in water;[48] thus, ΔS_{II} is the local entropy change for turning a water molecule into an ion. In the present study, $s^{ex}_{es,loc}$ is the entropy change for turning the LJ particle into an ion that interacts with waters with local electrostatic interactions. Because the entropy of liquid water, obtained from the enthalpy[55] and free energy[56] difference, is about −12 cal/(mol K) and similar values are obtained for the LJ particles employed here, a correspondence between ΔS_{II} and $s^{ex}_{es,loc}$ can be expected.[48]

We see the present development as placing these previously discussed local models of ion hydration entropies on a more quantitative footing; the energetic partitioning employed here provides a physical separation into local (first-shell) and far-field (outer-shell) parts and provides a clear thermodynamic signature of the often-used terms kosmotrope (strongly hydrated ion) and chaotrope (weakly hydrated ion).[9] Kosmotropes display negative $s^{ex}_{es,loc}$ values while chaotropes exhibit positive values. The results discussed above suggest that the F^- and Na^+ ions are kosmotropes, the Cl^- ion is neutral, K^+ is a weak chaotrope, and the larger halides are chaotropes. This interpretation is consistent with discussions of the Hofmeister series,[45,57] in which the Cl^- is often viewed as the transition ion between the two limits along the anion series. Figure 2 plots $s^{ex}_{es,loc}$ and $s^{ex}_{es,far}$ vs the inverse of the ion size (taken as the Pauling crystal radius[58]); for the anion

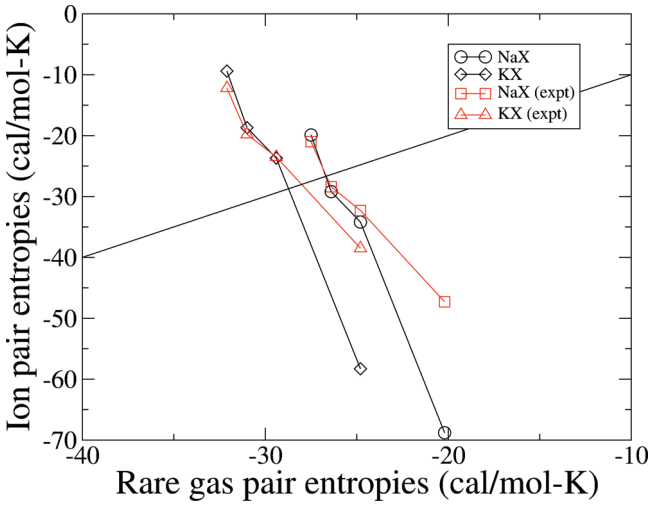

Figure 3. Comparison of the computed total entropies for the KX (left) and NaX (right) series, where X = F^-, Cl^-, Br^-, and I^-. The points for the F^- ion are on the bottom of each curve. Experimental data from Ben-Naim[4] was used for the rare gas entropies for both the theoretical and experimental plots. The experimental ion data was also taken from ref 4. The computed entropies are in black, while experimental values are in red. The diagonal line reflects a direct correlation. The modeled I_g^- ion is omitted from the plot.

series, the local electrostatic entropy displays a roughly linear correlation with the inverse of the ion size. Such behavior should be viewed only as an interesting correlation, however, because it has been shown that Gaussian models are not accurate for the local electrostatic contribution to the free energy.[27] Powell and Latimer[59] have presented an alternative correlation for the total hydration entropies based on charge−dipole interactions. It is interesting to note that, even though the K^+ and F^- ions are of comparable size, the cation displays a significantly more positive $s^{ex}_{es,loc}$ value, suggesting cations are inherently more chaotropic for a fixed ion size. Note also the weak size dependence of the far-field electrostatic contributions.

Finally, Figure 3 shows a plot of the computed total entropies vs experimental entropies for the isoelectronic rare gases for the NaX and KX series. A clear inverse correlation is observed, consistent with the above discussion; hydration entropy magnitudes increase with rare gas size but decrease with ion size. The KCl case lies relatively close to the diagonal. Even though the relatively close correspondence between ion and rare gas hydration entropies (in the sense that they are both negative and relatively small in magnitude) has continued to provide an interesting and counterintuitive example of subtleties in hydration problems,[7] the case of KCl[1,2] is in some sense misleading because it is near the crossing point of the observed and diagonal curves; the NaBr and NaI data lie similarly close to the diagonal. Except for the pairs involving the F^- ion, the agreement between theory and experiment is quite good.

CONCLUSIONS

To summarize, ion hydration entropies have been analyzed by energetic partitioning of the potential distribution theorem free energy. The computed vdW parts of the hydration entropy follow the expected trend of more negative values with increasing particle size. The far-field electrostatic component of the entropy does not show extensive ion specificity and is consistent with simple dielecric models in that small magnitude negative values are observed for all ions. The local electrostatic part of the entropy, however, provides a clear signature of the nature of the water ordering or disordering around the ion. The sign of this contribution yields a quantitative measure of the kosmotropic/chaotropic distinction[9,48] in ion hydration: ions with negative values are kosmotropes while ions with positive values are chaotropes. The findings provide a thermodynamic connection to spectroscopic experiments,[47] and a range of other experiments,[45,48] that suggest the ions influence water structure in a substantial way only locally. The conclusions are also consistent with an alternative statistical mechanical analysis of ion hydration free energies.[60] Future work will examine further the influence of ion size, charge, and polarization on the computed entropies,[49] hydration entropies of molecular ions, and the behavior of the various parts of the entropy near aqueous interfaces and protein fragments.

AUTHOR INFORMATION

Corresponding Author

*E-mail: thomas.beck@uc.edu.

ACKNOWLEDGMENT

This research was supported by NSF Grant Nos. CHE-0709560 and CHE-1011746. I would like to thank Lawrence Pratt, John Weeks, Dor Ben-Amotz, Barry Ninham, Kim Collins, Paul Cremer, Yizhak Marcus, and David Rogers for helpful discussions. I thank the Ohio Supercomputer Center for a generous grant of computer time and the Ponder group for the availability of the Tinker molecular dynamics code on their webpage. The present study was motivated by comments made by Lawrence Pratt at a 2010 Telluride Workshop on ions in chemistry and biology. In particular, he presented the experimental data corresponding to the computed results presented in Figure 3.

REFERENCES

(1) Robinson, R. A.; Stokes, R. H. *Electrolye Solutions*; Dover: New York, 1959.
(2) Friedman, H. L.; Krishnan, C. V. Thermodynamics of Ion Hydration. In *Water: A Comprehensive Treatise*; Franks, F., Ed.; Plenum Press: New York, 1973.
(3) Marcus, Y. *Ion Solvation*; John Wiley: New York, 1985.
(4) Ben-Naim, A. *Solvation thermodynamics*; Plenum Press: New York, 1987.
(5) Krestov, G. A. *Thermodynamics of Solvation*; Ellis Horwood: New York, 1991.
(6) Schmid, R.; Miah, A. M.; Sapunov, V. N. *Phys. Chem. Chem. Phys.* **2000**, *2*, 97–102.
(7) Ben-Amotz, D.; Underwood, R. *Acc. Chem. Res.* **2008**, *41*, 957–967.
(8) Marcus, Y. *Chem. Rev.* **2009**, *109*, 1346–1370.
(9) Ninham, B. W.; Lo Nostro, P. *Molecular Forces and Self Assembly*; Cambridge University Press: Cambridge, U.K., 2010.
(10) Irudayam, S. J.; Henchman, R. H. *Mol. Phys.* **2011**, *109*, 37–48.
(11) Asthagiri, D.; Pratt, L. R.; Paulaitis, M. E.; Rempe, S. B. *J. Am. Chem. Soc.* **2004**, *126*, 1285–1289.
(12) Asthagiri, D.; Pratt, L.; Kress, J. *Proc. Natl. Acad. Sci. U.S.A.* **2005**, *102*, 6704–6708.
(13) Asthagiri, D.; Pratt, L.; Kress, J. *Phys. Rev. E* **2003**, *68*, 041505.
(14) Paliwal, A.; Asthagiri, D.; Pratt, L. R.; Ashbaugh, H. S.; Paulaitis, M. E. *J. Chem. Phys.* **2006**, *124*, 224502.
(15) Shah, J. K.; Asthagiri, D.; Pratt, L. R.; Paulaitis, M. E. *J. Chem. Phys.* **2007**, *127*, 144508.

(16) Asthagiri, D.; Pratt, L.; Kress, J.; Gomez, M. *Proc. Natl. Acad. Sci. U.S.A.* **2004**, *101*, 7229–7233.
(17) Rempe, S.; Asthagiri, D.; Pratt, L. R. *Phys. Chem. Chem. Phys.* **2004**, *6*, 1966–1969.
(18) Asthagiri, D.; Dixit, P.; Merchant, S.; Paulaitis, M.; Pratt, L.; Rempe, S.; Varma, S. *Chem. Phys. Lett.* **2010**, *485*, 1–7.
(19) Varma, S.; Rempe, S. B. *J. Am. Chem. Soc.* **2008**, *130*, 15405–15419.
(20) Beck, T. L.; Paulaitis, M. E.; Pratt, L. R. *The Potential Distribution Theorem and Models of Molecular Solutions*; Cambridge University Press: New York, 2006.
(21) Rodgers, J.; Kaur, C.; Chen, Y.; Weeks, J. *Phys. Rev. Lett.* **2006**, *97*, 097801.
(22) Rodgers, J.; Weeks, J. *Proc. Natl. Acad. Sci. U.S.A.* **2008**, *105*, 19136–19141.
(23) Rodgers, J.; Weeks, J. *J. Phys.: Condens. Matter* **2008**, *20*, 494206.
(24) Rodgers, J.; Weeks, J. *J. Chem. Phys.* **2009**, *131*, 244108.
(25) Hu, Z.; Weeks, J. *Phys. Rev. Lett.* **2010**, *105*, 140602.
(26) Widom, B. *J. Phys. Chem.* **1982**, *86*, 869–872.
(27) Beck, T. L. *J. Stat. Phys.* **2011**in press.
(28) Chipot, C.; Pohorille, A. In *Free Energy Calculations: Theory and Applications in Chemistry and Biology*; Chipot, C., Pohorille, A., Eds.; Springer-Verlag: Berlin, 2007; pp 33−75.
(29) Bennett, C. H. *J. Comput. Phys.* **1976**, *22*, 245–268.
(30) Ben-Amotz, D.; Raineri, F. O.; Stell, G. *J. Phys. Chem. B* **2005**, *109*, 6866–6878.
(31) Hummer, G.; Pratt, L. R.; Garcia, A. E. *J. Phys. Chem.* **1996**, *100*, 1206–1215.
(32) Whitfield, T. W.; Varma, S.; Harder, E.; Lamoureux, G.; Rempe, S. B.; Roux, B. *J. Chem. Theor. Comput.* **2007**, *3*, 2068–2082.
(33) Baer, M. D.; Mundy, C. J. *J. Phys. Chem. Lett.* **2011**, *2*, 1088–1093.
(34) Ren, P.; Ponder, J. W. *J. Phys. Chem. B* **2003**, *107*, 5933–5947.
(35) Ponder, J.; Wu, C.; Ren, P.; Pande, V.; Chodera, J.; Schnieders, M.; Haque, I.; Mobley, D.; Lambrecht, D.; DiStasio, R.; Head-Gordon, M.; Clark, G.; Johnson, M.; Head-Gordon, T. *J. Phys. Chem. B* **2010**, *114*, 2549–2564.
(36) Rogers, D. M.; Beck, T. L. *J. Chem. Phys.* **2010**, *132*, 014505.
(37) Zhao, Z.; Rogers, D. M.; Beck, T. L. *J. Chem. Phys.* **2010**, *132*, 014502.
(38) Ben-Amotz, D. *J. Phys. Chem. Lett.* **2011**, *2*, 1216–1222.
(39) Warren, G. L.; Patel, S. *J. Chem. Phys.* **2007**, *127*, 064509.
(40) Carlsson, J.; Aqvist, J. *J. Phys. Chem. B* **2009**, *113*, 10255–10260.
(41) Horinek, D.; Herz, A.; Vrbka, L.; Sedlmeier, F.; Mamatkulov, S. I.; Netz, R. R. *Chem. Phys. Lett.* **2009**, *479*, 173–183.
(42) Rogers, D. M.; Beck, T. L. *J. Chem. Phys.* **2008**, *129*, 134505.
(43) Asthagiri, D.; Merchant, S.; Pratt, L. R. *J. Chem. Phys.* **2008**, *128*, 244512.
(44) Ashbaugh, H. S.; Pratt, L. R. *Rev. Mod. Phys.* **2006**, *78*, 159–178.
(45) Collins, K. D.; Washabaugh, M. W. *Q. Rev. Biophys.* **1985**, *4*, 323–422.
(46) Moessner, R.; Ramirez, A. P. *Phys. Today* **2006**, *59* (2), 24–29.
(47) Omta, A. W.; Kropman, M. F.; Woutersen, S.; Bakker, H. J. *Science* **2003**, *301*, 347–349.
(48) Collins, K. D.; Neilson, G. W.; Enderby, J. E. *Biophys. Chem.* **2007**, *128*, 95–104.
(49) Lynden-Bell, R. M.; Rasaiah, J. C. *J. Chem. Phys.* **1997**, *107*, 1981–1991.
(50) Frank, H. S.; Evans, M. W. *J. Chem. Phys.* **1945**, *13*, 507–532.
(51) Ashbaugh, H.; Asthagiri, D.; Pratt, L.; Rempe, S. *Biophys. Chem.* **2003**, *105*, 323–338.
(52) Thompson, W. H.; Hynes, J. T. *J. Am. Chem. Soc.* **2000**, *122*, 6278–6286.
(53) Horvath, S.; Mccoy, A.; Roscioli, J.; Johnson, M. *J. Phys. Chem. A* **2008**, *112*, 12337–12344.
(54) Perera, P. N.; Browder, B.; Ben-Amotz, D. *J. Phys. Chem. B* **2009**, *113*, 1805–1809.
(55) Stern, H. A.; Berne, B. J. *J. Chem. Phys.* **2001**, *115*, 7622–7628.
(56) Weber, V.; Asthagiri, D. *J. Chem. Phys.* **2010**, *133*, 141101.
(57) Zhang, Y.; Cremer, P. *Annu. Rev. Phys. Chem.* **2010**, *61*, 63–83.
(58) Pauling, L. *The Nature of the Chemical Bond*; Cornell University Press: Ithaca, NY, 1960.
(59) Powell, R. E.; Latimer, W. M. *J. Chem. Phys.* **1951**, *19*, 1139–1141.
(60) Merchant, S.; Asthagiri, D. *J. Chem. Phys.* **2009**, *130*, 195102.
(61) Smith, D. J.; Saykally, R. J.; Geissler, P. L. *J. Am. Chem. Soc.* **2007**, *129*, 13847–13856.

NOTE ADDED IN PROOF

The Raman spectroscopy experiments in ref 61 lead to similar conclusions to those presented in ref 47.